Published in Optics Letters 24, 866 (1999)

Polarized light scattering measurements of dielectric spheres on a silicon surface

Lipiin Sung

National Institute of Standards and Technology, Gaithersburg, MD 20899

University of Maryland, College Park, MD 20742

George W. Mulholland and Thomas A. Germer

National Institute of Standards and Technology, Gaithersburg, MD 20899

ABSTRACT

The polarization of light scattered into directions out of the plane of incidence by polystyrene latex spheres on a silicon substrate was measured for p-polarized incident light. The experimental data show good agreement with theoretical predictions for three sizes of spheres. These results demonstrate that the polarization of light scattered by particles can be used to determine the size of particulate contaminants on silicon wafers. Theoretical models, based on successive degrees of approximation, indicate that the mean distance of a particle from the surface is the primary determinant of the scattered light polarization for small out-of-plane scattering angles.

Detection and characterization of particles and defects on surfaces have been of great interest to the optical and semiconductor industries. Instruments based upon light scattering satisfy many of the requirements of the industry, such as high throughput rate and high sensitivity. However, scattered light may arise from a number of different sources, such as surface topography, surface residue, particulate contamination, and subsurface defects. Analyzing the scattered intensity to correctly determine the size, shape, and material of a contaminant is complicated. Recently, Germer *et al.*[1–3] have demonstrated experimentally and theoretically that the polarization of scattered light can be used to distinguish amongst various types of light scattering features near surfaces. Using the unique polarization properties of each scatter source, one can separate the contribution from the various sources of scattering, and improve the ability of optical inspection tools to detect particulate contamination and subsurface defects over a background dominated by substrate microroughness.

In this paper, we present a model system containing accurately-sized polystyrene latex (PSL) spheres on a silicon surface to test theoretical models for scattering from particles above a surface. Numerous theories describing the light (of wavelength λ) scattered by a sphere of diameter D and complex refractive index n_{sph} above a smooth surface of complex refractive index n_{s} have been developed. [1,4–8] In the Rayleigh approximation,[1,6,7] valid for $D << \lambda$, the scatterer is treated as a point polarizable dipole. The particle is assumed to be illuminated by the incident light and by its reflection in the surface, and the induced dipole is assumed to radiate directly into the scattering hemisphere and through reflection in the surface. The key parameter in this approximation is the mean distance $d = D/2$ of the particle from the surface, which determines the interference between the different optical paths.

The PSL spheres we used in this study are sufficiently large that the light scattered from an isolated sphere is not entirely Rayleigh-like. In the Mie-surface approximation (sometimes referred to as the double interaction model[8]), we include the field scattered by a homogeneous sphere, using the exact Mie solution[9] for a sphere in free space. In both the Rayleigh and Mie-surface approximations, we neglect the interaction between the particle and its image in the substrate. To account for this interaction, a discrete-dipole approximation (DDA) is used. In the DDA, an object is built out of a large number of interacting dipoles. The near field interactions between each dipole, both directly and through their reflections in the surface, are included in the calculation. A self-consistent solution for all the dipoles is iteratively determined. A complete description of the DDA algorithm is described elsewhere.[10] In all the approximations, it is assumed that the spheres are isolated.

A low-pressure impactor connected to a particle generation/classification system was used to deposit monodisperse PSL spheres onto bare silicon wafers.[11,12] Results for PSL spheres, having diameters (100.7 ± 1.0) nm, (181.0 ± 6.0) nm, and (217.7 ± 3.4) nm[12,13] and polydispersity less than 2 %, will be presented in this paper. Using a dark field reflection optical microscope, we estimated the number density of the samples containing 181.0 nm and 217.7 nm spheres to be about 0.03 μm^{-2} in the illuminated sample regions. Less than 2 % of the particles were doublets. A field emission scanning electron microscope indicated that about 10 % of particles deposited on the sample containing 100.7 nm spheres were doublets and that the number density was about 0.2 μm^{-2}. The effect of the presence of doublets on the polarization of scattered light will be discussed later in the text.

Figure 1(a) shows the optical geometry used in this study. Laser light of wavelength $\lambda = 532$ nm is incident onto a sample (Gaussian beam diameter $2w_0 \approx 1$ mm) at an angle $\theta_{\rm i}$, and light scattered into a solid angle $\Omega \approx 10^{-4}$ sr centered on a polar angle

θ_r and azimuthal (out-of-plane) angle ϕ_r is collected. Bidirectional ellipsometric (BE) measurements are presented in terms of the principal angle of polarization, $\eta^{(\mathrm{p})}$, and the degree of linear polarization, $P_\mathrm{L}^{(\mathrm{p})}$, as functions of ϕ_r for fixed θ_i and θ_r for p-polarized incident light [see Fig. 1(b)]. The bidirectional reflectance distribution functions (BRDF) levels in the $\theta_\mathrm{i} = \theta_\mathrm{r} = 45°$ and $\phi_\mathrm{r} = 90°$ configuration were approximately 1×10^{-4} sr^{-1}, 2×10^{-5} sr^{-1}, 4×10^{-6} sr^{-1}, and 1×10^{-7} sr^{-1}, for samples with 217.7 nm, 181.0 nm, and with 100.7 nm spheres, and for the bare silicon wafers before deposition, respectively.

Figures 2(a)-(b) compare the predictions of the three models for the BE parameters for two particle sizes, 100 nm and 200 nm. In all theoretical calculations performed in this study, we assume indices of refraction appropriate for $\lambda = 532$ nm: $n_\mathrm{sph} = 1.59$ and $n_\mathrm{s} = 4.15 + 0.05\,i$. By comparing the predictions of the three approximations, we can evaluate the contributions from the interference between the incident and the reflected beams (from the Rayleigh model), the finite size and the material of the sphere (from the differences between the Rayleigh and the Mie-surface models) and the near field sphere-surface interaction (from the differences between the Mie-surface and DDA models). Note that the differences between the models become noticeable as the particle diameter increases. However, the predictions for $\eta^{(\mathrm{p})}$ at small ϕ_r (for $\phi_\mathrm{r} \leq 60°$) are relatively independent of the model. This finding indicates that the strongest determining factor of the parameter $\eta^{(\mathrm{p})}$ at small ϕ_r is the mean distance of the sphere from the surface, and is not strongly affected by the material of the sphere.

It is evident that $\eta^{(\mathrm{p})}$ has a unique angular dependence for each particle size, and that we can relate the slope of the $\eta^{(\mathrm{p})}$ vs. ϕ_r curves near $\phi_\mathrm{r} = 0$ to the particle size. Figure 2(c) shows $-\Delta\eta^{(\mathrm{p})}/\Delta\phi_\mathrm{r}$, evaluated at $\phi_\mathrm{r} = 0$, as a function of the diameter of the particle for the three different approximations. All three models predict similar behaviors in the displayed region, and converge to each other for small diameters. This result implies that the particle size can be estimated by the slope of $\eta^{(\mathrm{p})}$ in the small

ϕ_r region, or more simply, by the value of $\eta^{(p)}$ at a small fixed ϕ_r. However, to determine the size of an arbitrary particle more accurately and to obtain information about particle-substrate interaction, the particle shape, or the particle material, we would need to measure the BE parameters for a wide range of ϕ_r, and for different θ_i and θ_r. Since the DDA model is the most complete model, we use it for the remainder of the paper to compare to the experimental data. Experimental data obtained from three particle sizes are also shown in Fig. 2(c) and will be discussed later in the text.

Figure 3 shows the BE parameters for the sample with 181.0 nm PSL spheres as functions of ϕ_r for different values of $\theta_i = \theta_r$, together with the corresponding theoretical predictions of the DDA model. The experimental data are in good agreement with the theoretical predictions for all values of ϕ_r at all scattering conditions. A more detailed examination of the data indicates that there is a slight deviation for large θ_i or θ_r. The differences between the data and the theory for large θ_i or θ_r may be due to contributions from interactions between particles, non-spherical particles on the surface, or from interference with other scattering sources. Random sources of scatter, such as these, are expected to depolarize the light.

Figure 4 shows the BE results at $\theta_i = \theta_r = 45°$ for samples with three different diameters. The DDA model predicts the overall trend of the angular dependence of the BE parameters for particles with different diameters. The agreement between the measured polarization angles $\eta^{(p)}$ and those predicted by the theory for a 217.7 nm PSL sphere is excellent. However, the corresponding values of measured $P_L^{(p)}$ are smaller than those predicted by the theory at large scattering angles. Again, the increasing depolarization of light may be due to the similar causes we mentioned previously. The results in Fig. 4 imply that we can determine the size of the spheres using BE measurements. We also extract the values of $-\Delta\eta^{(p)}/\Delta\phi_r$ ($\phi_r \to 0$), and present the results with the theoretical predictions in Fig. 2(c). The uncertainties of $-\Delta\eta^{(p)}/\Delta\phi_r$ were evaluated by a standard statistical data analysis from the linear regression of the first few data in the $\eta^{(\mathrm{p})}$ vs. ϕ_{r} plot [see Fig. 2(c)] and represent 95 % confidence levels. These results in Fig. 2(c) suggest that we can use BE data in small out-of-plane scattering angles to estimate the size of unknown spheres.

While the agreement between theory and experimental data in Figs. 2(c) and 4 is good for the 181.0 nm and 217.7 nm spheres, it is not as good for the 100.7 nm spheres. The discrepancies between the data and theory, for the sample containing 100.7 nm PSL spheres are probably due to contributions from doublets. We calculated the BE parameters for systems with two touching 100.7 nm spheres, aligned along the $\hat{\boldsymbol{x}}$, $\hat{\boldsymbol{y}}$, and $\hat{\boldsymbol{z}}$ directions. It is found that $-\Delta\eta^{(\mathrm{p})}/\Delta\phi_{\mathrm{r}}$ for these systems is about 1.1 times, 2.3 times, and 2.8 times larger, respectively, than that from a system with a single sphere. Without accurate information about the density and geometrical configurations of the doublets, it is difficult to further refine the model to account for the presence of doublets. Further work will be carried out to reduce the fraction of such doublets.

In summary, BE measurements of a model system containing accurately-sized PSL spheres on silicon were made and compared to a DDA model for a sphere above a smooth surface. This study demonstrates that the polarization of light scattered by particles can be used to determine the size of particulate contaminants on a smooth surface.

The authors would like to thank Dr. John Small and Mr. Marco Fernandez for assisting in some associated measurements.

Figure Captions

Figure 1 (a) The optical geometry used in this paper; (b) a schematic polar plot of the intensity distribution f measured by a rotating linear-polarization-sensitive detector, defining the BE parameters, $\eta^{(\mathrm{p})}$ and $P_{\mathrm{L}}^{(\mathrm{p})} = (f_{\mathrm{max}} - f_{\mathrm{min}})/(f_{\mathrm{max}} + f_{\mathrm{min}})$.

Figure 2 (a)-(b) Results of BE calculations using three approximations for light scattering from two different diameters of PSL spheres above a smooth silicon surface for $\lambda = 532$ nm at $\theta_{\mathrm{i}} = \theta_{\mathrm{r}} = 45°$. (c) The slope, $-\Delta\eta^{(\mathrm{p})}/\Delta\phi_{\mathrm{r}}$ ($\phi_{\mathrm{r}} \rightarrow 0$), as a function of D for three theoretical approximations with experimental results.

Figure 3 BE parameters for 181.0 nm PSL spheres on silicon at different incident and scattering angles. The curves represent the predictions of the DDA model. The uncertainties in the data are smaller or about the same size as the symbols.

Figure 4 Same as Fig. 3 except for three PSL sphere sizes at $\theta_{\mathrm{i}} = \theta_{\mathrm{r}} = 45°$.

References

[1]T. A. Germer, Appl. Opt. **36**, 8798 (1997).

[2]T. A. Germer, C. C. Asmail, and B. W. Scheer, Opt. Lett. **22**, 1284 (1997).

[3]T. A. Germer, and C. C. Asmail, Proc. SPIE **3121**, 173 (1997); *ibid.* **3141**, 220 (1997).

[4]G. Videen, J. Opt. Soc. Am. A**8**, 483 (1991); *ibid.* **9**, 844 (1992).

[5]P. A. Bobbert, and J. Vlieger, Physica A **137**, 209 (1986).

[6]W. S. Bickel, A. J. Watkins, and G. Videen, Am. J. Phys. **55**, 559 (1987).

[7]G. Videen, W. L. Wolfe and W. S. Bickel, Opt. Eng. **31**, 341 (1992).

[8]K. B. Nahm, and W. L. Wolfe, Appl. Opt. **26**, 2995 (1987); we do not include their shadow factor.

[9]F. C. Bohren and D. R. Huffman, *Absorption and Scattering of Light by Small Particles* (Wiley, New York, 1983).

[10]R. Schmehl, B. M. Nebeker, and E. D. Hirleman, J. Opt. Soc. Am. A**14**, 3026 (1997).

[11]S. V. Hering, S. K. Friedlander, J. J. Collins, and L. W. Richards, Env. Sci. Technol. **13**, 184 (1979).

[12]P. D. Kinney, D. Y. H. Pui, G. W. Mulholland, and N. P. Bryner, J. Res. Natl. Inst. Stand. Technol. **96**, 147 (1991).

[13] G. W. Mulholland, N. P. Bryner, and C. Croarkin, "Measurement of 100 nm NIST SRM 1963 by differential mobility analysis," J. Aersol Sci. and Technol., in press (1999).

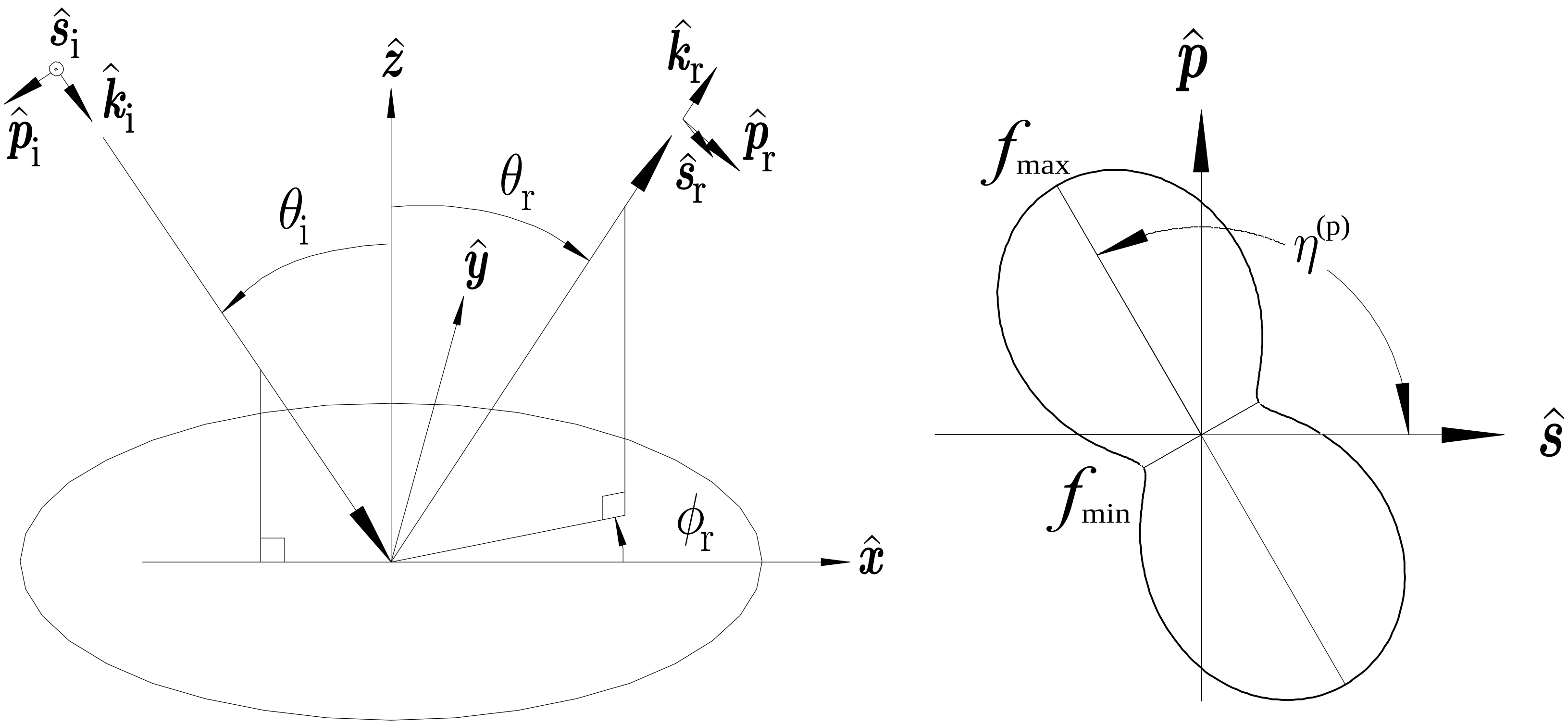

Sung et al., Figure 1

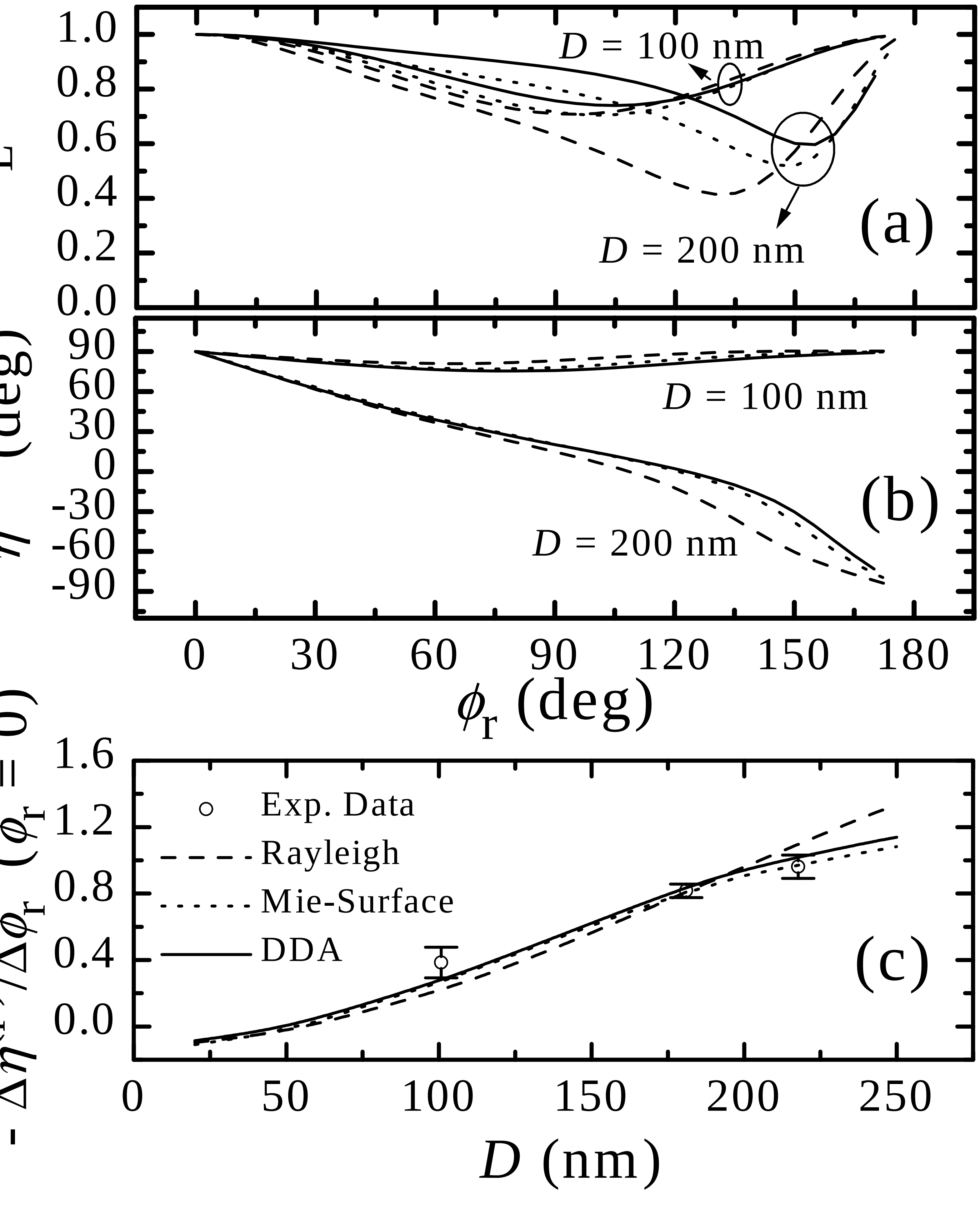

Sung et al., Figure 2

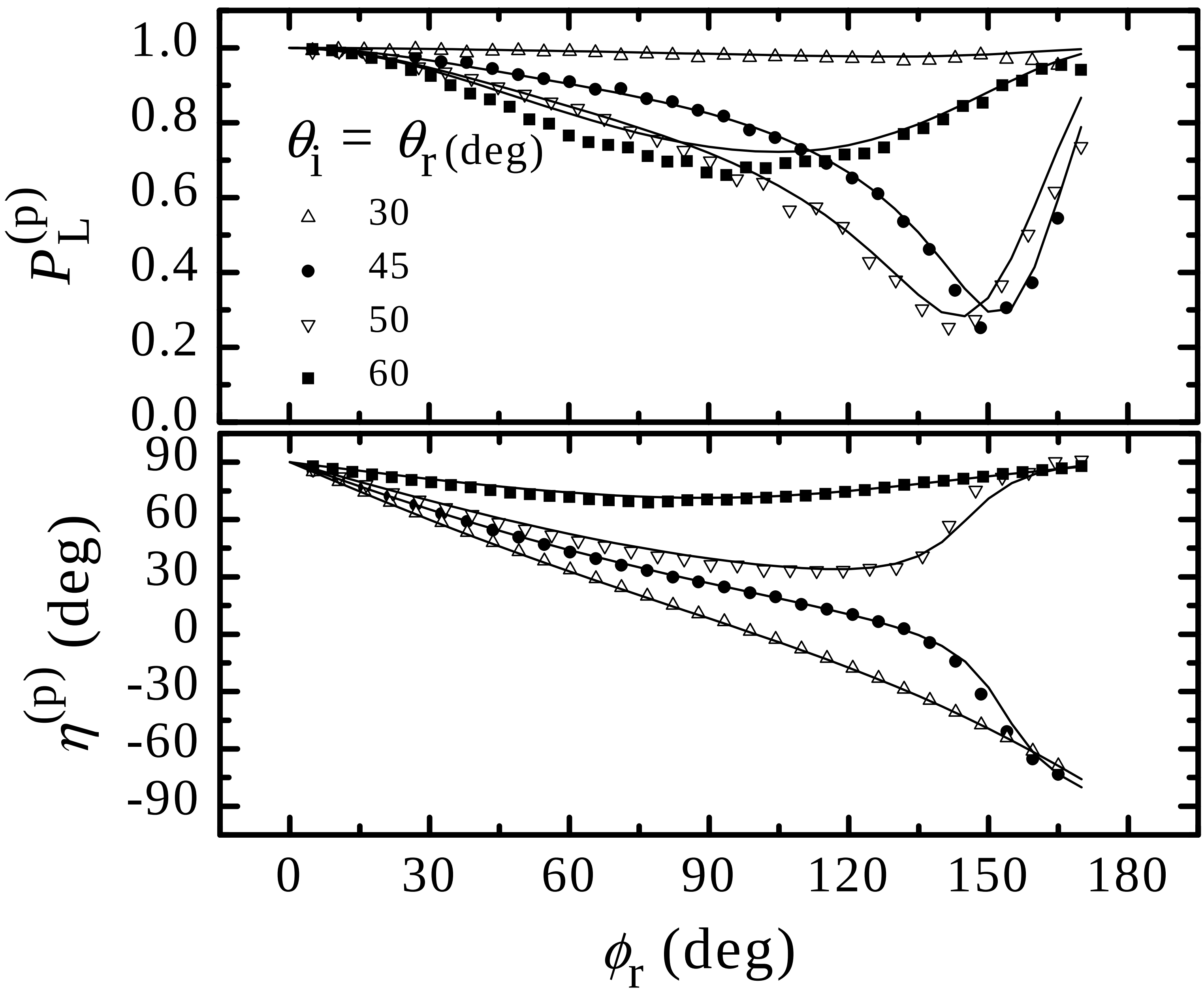

Sung et al., Figure 3

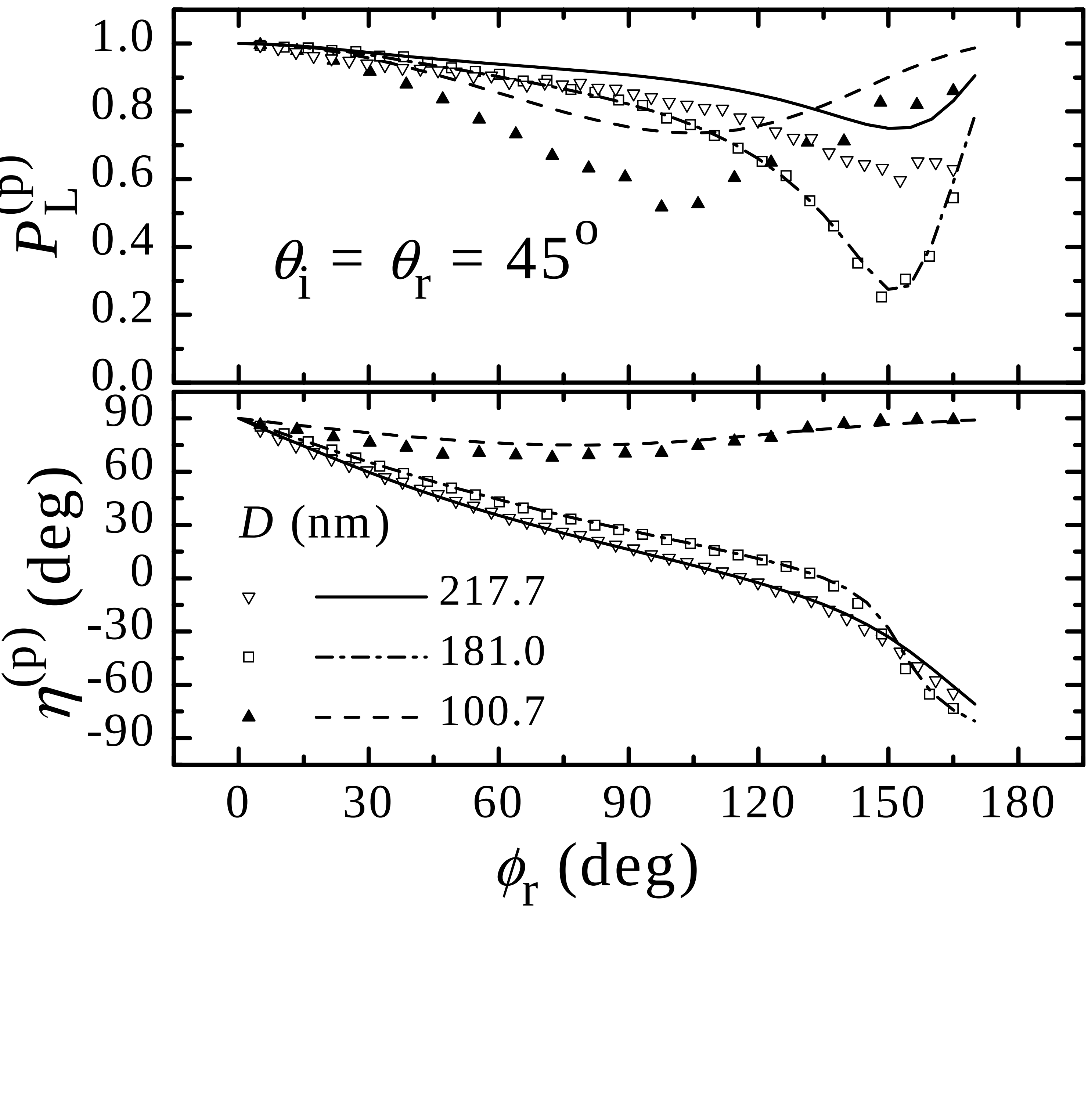

Sung et al., Figure 4